DYNAMIC PROPERTIES OF POLY (METHYLMETHACRYLATE) (PMMA) (PLEXIGLAS)

by

D. R. Christman

Materials and Structures Laboratory
Manufacturing Development, General Motors Corporation
General Motors Technical Center, Warren, Michigan 48090

UNCLASSIFIED
Security Classification

DOCUMENT CONTROL DATA - R & D

(Security classification of title, body of abstract and indexing annotation must be entered when the overall report is classified)

1. ORIGINATING ACTIVITY *(Corporate author)*: Manufacturing Development, General Motors Corporation, GM Technical Center, Warren, Michigan 48090

2a. REPORT SECURITY CLASSIFICATION: UNCLASSIFIED

2b. GROUP:

3. REPORT TITLE: Dynamic Properties of Poly(methylmethacrylate) (PMMA) (Plexiglas)

4. DESCRIPTIVE NOTES *(Type of report and inclusive dates)*: Final Report

5. AUTHOR(S) *(First name, middle initial, last name)*: Douglas R. Christman

6. REPORT DATE	7a. TOTAL NO OF PAGES	7b. NO OF REFS
1972 March	48	36

8a. CONTRACT OR GRANT NO	9a. ORIGINATOR'S REPORT NUMBER(S)
DASA01-68-C-0114	MSL-71-24
b. PROJECT NO: NWER Code XAXA	
c. Task & Subtask Code A106	9b. OTHER REPORT NO(S) *(Any other numbers that may be assigned this report)*: DNA 2810F
d. Work Unit Code 07	

10. DISTRIBUTION STATEMENT: Approved for public release; distribution unlimited.

11. SUPPLEMENTARY NOTES	12. SPONSORING MILITARY ACTIVITY
	Director Defense Nuclear Agency Washington, D. C. 20305

13. ABSTRACT

Results of an experimental study on the dynamic properties of poly(methylmethacrylate) are presented. Areas studied included uniaxial stress behavior, elastic constants, equation of state, compressive and release wave characteristics, and spall fracture. The material showed viscoelastic response under uniaxial stress conditions, and was strain rate sensitive at 20° and 82°C. Longitudinal and shear wave velocities at 20°C were 2.746 and 1.392 mm/μsec, and temperature dependence was also measured. The shock wave equation of state was determined up to 20 kbar and showed a complex form in the stress-particle velocity plane that is indicative of non-linear shock velocity-particle velocity behavior. Complete wave profiles were obtained showing compressive wave and release wave development. Spall fracture velocity showed a slight pulse-width dependence and the fracture surface showed a granular-type appearance with extensive crazing.

DD FORM 1 NOV 65 1473

14. KEY WORDS	LINK A		LINK B		LINK C	
	ROLE	WT	ROLE	WT	ROLE	WT
Stress-Strain-Strain Rate Elastic Constants Equation of State Compressive and Release Wave Characteristics Spall Fracture						

DNA 2810F
MSL-71-24
1972, March

DYNAMIC PROPERTIES OF POLY (METHYLMETHACRYLATE) (PMMA) (PLEXIGLAS)

" This work was supported by the Defense Nuclear Agency under NWER Subtask AA 106"

by

D. R. Christman

Materials and Structures Laboratory
Manufacturing Development, General Motors Corporation
General Motors Technical Center, Warren, Michigan 48090

Prepared For

HEADQUARTERS
Defense Nuclear Agency
Washington, D.C. 20305

Under Contract DASA01-68-C-0114

MSL-71-24

ABSTRACT

Results of an experimental study on the dynamic properties of poly(methylmethacrylate) are presented. Areas studied included uniaxial stress behavior, elastic constants, equation of state, compressive and release wave characteristics, and spall fracture. The material showed viscoelastic response under uniaxial stress conditions, and was strain rate sensitive at 20° and 82°C. Longitudinal and shear wave velocities at 20°C were 2.746 and 1.392 mm/μsec, and temperature dependence was also measured. The shock wave equation of state was determined up to 20 kbar and showed a complex form in the stress-particle velocity plane that is indicative of non-linear shock velocity-particle velocity behavior. Complete wave profiles were obtained showing compressive wave and release wave development. Spall fracture velocity showed a slight pulse-width dependence and the fracture surface showed a granular-type appearance with extensive crazing.

TABLE OF CONTENTS

LIST OF ILLUSTRATIONS

LIST OF TABLES

INTRODUCTION

This study of poly(methylmethacrylate) (PMMA) was conducted under the PREDIX program initiated by the Defense Nuclear Agency.[1] The program was concerned primarily with the response of metals under impulsive loading conditions but some tests were performed on PMMA to provide data on a viscoelastic, polymeric material. Although the tests were not as extensive as those conducted on 6061-T6 aluminum,[2] alpha titanium,[3] OFHC copper,[4] and tantalum,[5] sufficient data were obtained in various areas of material response to warrant preparation of a separate report.

The primary areas studied were: (1) uniaxial stress behavior; (2) elastic constants; (3) equation of state; (4) shock wave profiles; and (5) spall fracture. The experimental techniques utilized in this study are reviewed in Reference 6. Briefly, the principal techniques applied were:

Stress-Strain Studies - A laboratory-type universal testing machine was used for rates < 0.1/sec, a medium strain rate machine for rates of 10^{-3}/sec to 10^{2}/sec, and a Hopkinson bar device for rates of about 10^{2} to 5×10^{3}/sec.

Elastic Constants - The pulse superposition method was used for measuring longitudinal and shear wave velocities as a function of temperature.

Equation of State - Gun-launched, flat-plate impact techniques were used to generate uniaxial strain conditions.

Velocities up to 0.6 mm/μsec were achieved with 63.5 mm and 102 mm single-stage compressed-gas guns. Hugoniot data were obtained with x-cut quartz gages.

Wave Propagation and Spall Fracture - Flat-plate impact techniques were also used. Wave profiles were measured with x cut quartz gages, laser velocity interferometer and magnetic foil gages.

MATERIAL PROPERTIES

Poly(methylmethacrylate) or PMMA is a cast thermoplastic acrylic polymer made from methyl methacrylate monomers. The material used for the tests reported here was Rohm and Haas Plexiglas II UVA, an ultraviolet absorbing grade.[7] The material was purchased as sheet stock in thicknesses of 1.6, 3.2, 12.7 and 25.4 mm. Unless noted, all data reported are for a test direction normal to the plane of the sheet.

The average measured density was 1.183 g/cc (0.0427 lb/in.^{3}). The material has a softening or heat-distortion temperature in the range of 95-105°C and a Rockwell hardness of M93.[7] Thermal analyses by Asay, et al.,[8] on cast Acrylux (Cadillac Plastic and Chemical Co.) rod gave the following:

Volume coefficient of thermal expansion, β:

$145 \times 10^{-6} + 1.4 \times 10^{-6}T$ /°C

(10 to 100°C)

Specific Heat, c_p:

$0.1974 + 0.00176T$ cal/g-°C

(-100 to 45°C)

The above give $\beta = 163 \times 10^{-6}$ and $c_p = 0.23$ at 20°C. Other data on PMMA give values of β as high as 240×10^{-6} and c_p as high as 0.35.[7,9]

SECTION I

UNIAXIAL STRESS BEHAVIOR

The uniaxial stress response of PMMA has been studied under several programs at General Motors Corporation. Results of these studies are given in References 10 to 14, and cover such areas as strain rate and temperature effects in compression and tension, fracture, specimen size effects, and the influence of prestraining (uniaxial stress) and preshocking (uniaxial strain) on stress-strain behavior. In addition, numerous papers have been published on deformation characteristics of PMMA (see, e.g., References 15 and 16).

The response of PMMA to uniaxial stress loading is viscoelastic with high strain rate sensitivity, as shown in Figure 1.* The low-strain modulus and the high-strain flow stress increase by a factor of two or more for a strain-rate increase of 0.003/sec to 1500/sec, and decrease correspondingly for a temperature increase of 22°C to 82°C.

PMMA exhibits significant stress relaxation in uniaxial stress, and a specimen loaded in compression to ∿ 1% strain at ∿ 10/sec relaxed from 2.34 kbar to 1.63 kbar in ∿ 0.025 sec.(11) Specimens loaded in compression at 2.5/sec to 99% of maximum stress and then unloaded showed no change in stress-strain response on subsequent reloadings.(11)

* The data in Figure 1 are for 9.5 mm dia. by 12.7 mm long cylinders machined from 12.7 mm dia. cast rod.

Uniaxial stress tests on unshocked (as-received) and shocked (uniaxial strain compressive loading to 5 kbar) specimens showed no differences in compressive stress-strain response for strain rates of 0.003/sec. to 1100/sec.[11]

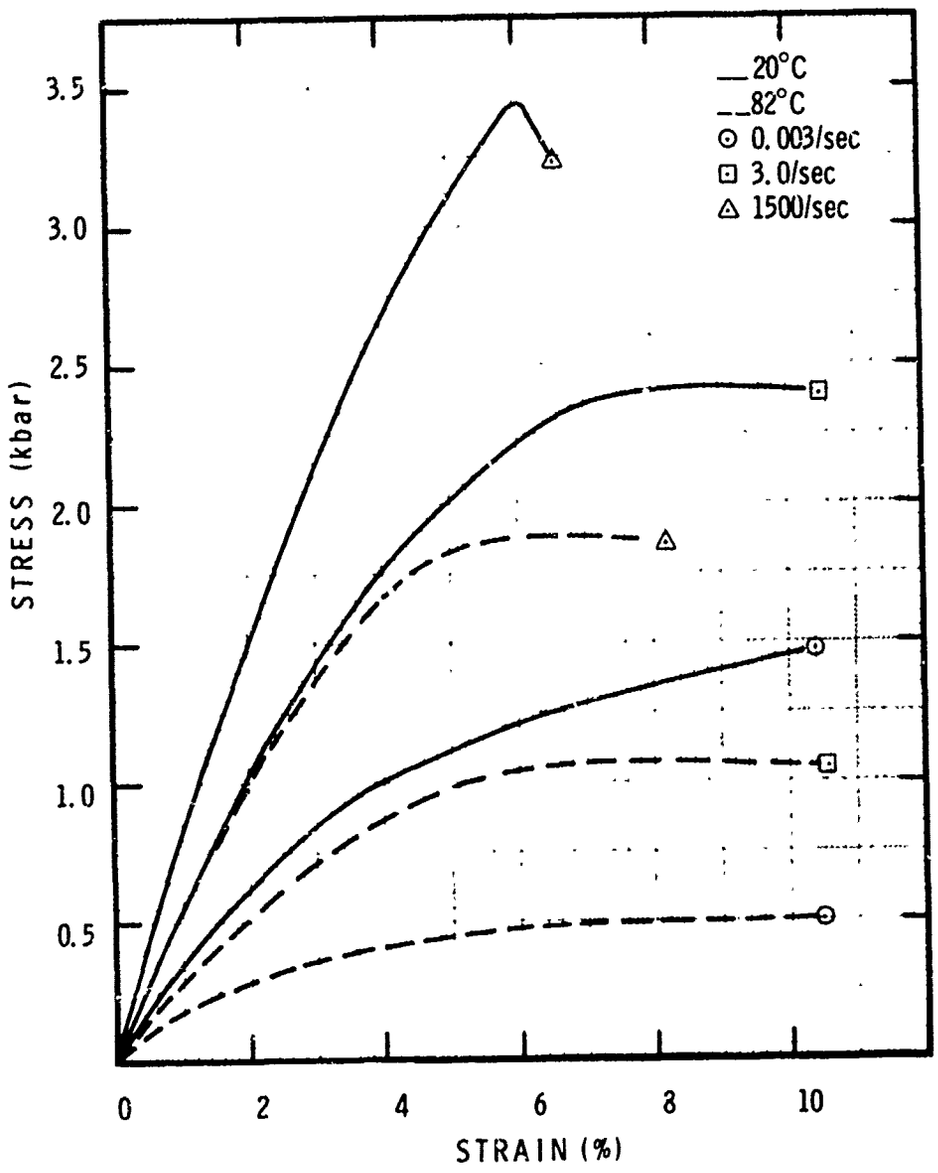

Figure 1 Compressive Stress vs. Strain, PMMA

SECTION II

ELASTIC BEHAVIOR

WAVE VELOCITIES

Measurements were made of longitudinal and shear wave velocities in PMMA at 20°C and atmospheric pressure (P = 0). Values obtained were:

$$\left.\begin{aligned} C_L &= 2.746 \pm 0.003 \text{ mm/}\mu\text{sec} \\ C_S &= 1.392 \pm 0.002 \text{ mm/}\mu\text{sec} \end{aligned}\right\} \quad (1)$$

The temperature dependence of C_L and C_S was also measured and, after correction for thermal expansion, gave:

$$\left.\begin{aligned} C_L &= 2.801 - 26.4 \times 10^{-4}T - 0.05 \times 10^{-4}T^2 \\ C_S &= 1.420 - 13.6 \times 10^{-4}T - 0.028 \times 10^{-4}T^2 \end{aligned}\right\} \quad (2)$$

(T in °C)

Asay, et al.,[8,17] measured the temperature dependence of C_L and C_S along the axial direction of cast PMMA rod and obtained values in reasonable agreement with those given above.

Asay, et al., [17] also reported the pressure dependence of C_L and C_S giving:

$$\left.\begin{aligned} C_L &= 2.7519 + 0.2452P - 0.0166P^2 + 0.000589P^3 \\ C_S &= 1.3977 + 0.0965P - 0.00705P^2 + 0.00270P^3 \end{aligned}\right\} \quad (3)$$

(P in kbar)

Note that the zero pressure values of C_L and C_S (2.7519 and 1.3977) are about ∿ 0.3% higher than those given in Equation 1 for material taken from sheet stock.

ELASTIC CONSTANTS

Assuming PMMA is homogeneous and isotropic, elastic wave velocity data can be used to calculate various elastic constants. At 20°C and zero pressure, the following adiabatic constants were obtained:

Bulk wave velocity, C_B = 2.23 mm/μsec

Sound wave velocity, C_E = 2.27 mm/μsec

Poisson's ratio, ν = 0.327

Bulk modulus, K = 58.6 kbar

Shear modulus, G = 22.9 kbar

Elastic modulus, E = 60.8 kbar

Lamé's parameter, λ = 43.4 kbar

Isothermal values of K and G as well as adiabatic and isothermal pressure and temperature derivatives at 20°C and zero pressure were calculated using pressure dependence, specific heat and thermal expansion data* reported by Asay, et al.[8,17] Results are given in Table I.

* Use of higher values for β and c_p than reported by Asay has a small effect on the calculations, with the results being 0.2 to 4% different for $\beta = 240 \times 10^{-6}$ and $c_p = 0.35$.

TABLE I

ELASTIC CONSTANTS FOR PMMA

(P = 0, T = 20°C)

PARAMETER	VALUE
K^S	58.6 kbar
$(\frac{\partial K^S}{\partial P})_T = K_{0T}^{S'}$	12.7
$(\frac{\partial K^S}{\partial T})_P$	- 0.129 kbar/°C
$(\frac{\partial K^S}{\partial P})_S = K_{0S}^{S'}$	12.2
$(\frac{\partial K^S}{\partial T})_S$	2.85 kbar/°C
K^T	56.4 kbar
$(\frac{\partial K^T}{\partial P})_T = K_{0T}^{T'}$	13.0
$(\frac{\partial K^T}{\partial T})_P$	- 0.151 kbar/°C
$(\frac{\partial K^T}{\partial P})_S = K_{0S}^{T'}$	12.4
$(\frac{\partial K^T}{\partial T})_S$	2.90 kbar/°C
$G^S = G^T$	22.9 kbar
$(\frac{\partial G}{\partial P})_T = G_{0T}^{'}$	3.58
$(\frac{\partial G}{\partial T})_P$	- 0.052 kbar/°C
$(\frac{\partial G}{\partial P})_S = G_{0S}^{'}$	3.36
$(\frac{\partial G}{\partial T})_S$	0.79 kbar/°C

SECTION III

EQUATION OF STATE

The hugoniot equation of state is the locus of equilibrium states reached after shock-loading of a material, and data are usually obtained either as stress-particle velocity points or as shock velocity-particle velocity points. The hugoniot data presented in this report were obtained with x-cut quartz gages and representative records for direct impact and transmitted wave tests are shown in Figure 2. The buffered direct impact method (tungsten carbide or 4340 steel buffer plate on front of the quartz) permitted stresses up to 20 kbar in PMMA while keeping impact velocity requirements within the capability of the 102 mm gun. The use of quartz gages for transmitted wave tests was primarily for the study of compressive wave development, and results are discussed in the Wave Propagation Section.

The hugoniot may be expressed in several forms and the most convenient form based on quartz gage results is that established by a least-squares fit to data in the stress-particle velocity (σ_H - u_p) plane. Results for PMMA are given in Figure 3 and the hugoniot is

$$\sigma_H = 29\ u_p + 80.3\ u_p^2 - 244.5\ u_p^3 + 256.4\ u_p^4 \qquad (4)$$

For metals, a second order equation is usually sufficient to give a reasonable fit to the data,[2-5] however, a fourth-order equation is given for PMMA for two reasons. First, the standard error for second and third-order fits is 0.1 kbar, while the fourth-order equation reduces this to 0.05 kbar. Second, the work of other investigators has established that

TIME ⟶

DIRECT IMPACT
PMMA → Qz
V_I = 0.122 mm/μs
σ_H = 3.40 kbar

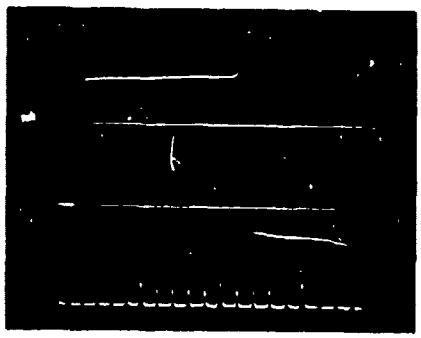

DIRECT IMPACT, BUFFERED
PMMA → 4340 ST./Qz
V_I = 0.163 mm/μs
σ_H = 5.55 kbar

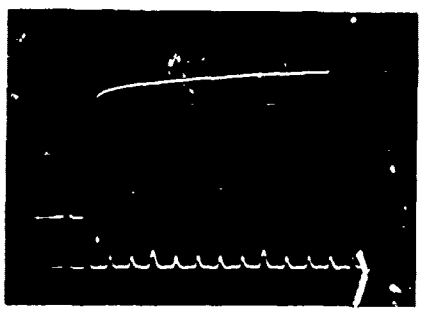

TRANSMITTED WAVE
6061-T6 Al → PMMA/Qz
V_I = 0.252 mm/μs
σ_H = 7.5 kbar

Figure 2 Quartz Gage Records

PMMA does not have a conventional hugoniot in the low-pressure region (see e.g., Refs. 18-22).* Also shown in Figure 3 are data of Barker and Hollenbach[21] which show good agreement with the present work.

Transformation of the hugoniot into other planes, such as stress-volume (σ_H - v) or shock velocity-particle velocity (U_S - u_p) is performed by assuming a material model. Since PMMA does not show an elastic-plastic structure, this was done by assuming an ideal single-wave structure with equilibrium initial and final states and applying the mass and momentum conservation equations:

$$\sigma_H = \rho_o U_S u_p$$

and

$$v = v_o \left(1 - \frac{u_p}{U_S}\right)$$

Results are given in Table II and Figures 4 and 5. Barker's data and fits[21] are also shown. The calculated shock velocities from the present work are slightly lower than Barker's measured values, but the agreement is good considering the assumption underlying the data transformation and the effects of material variability and experimental error. Shock velocities measured on three transmitted wave tests are also given in Figure 5.

---

* Deal[23] did a review paper on all the data available up to 1965 on PMMA-type materials, but the data scatter did not permit resolution of details of low-pressure response.

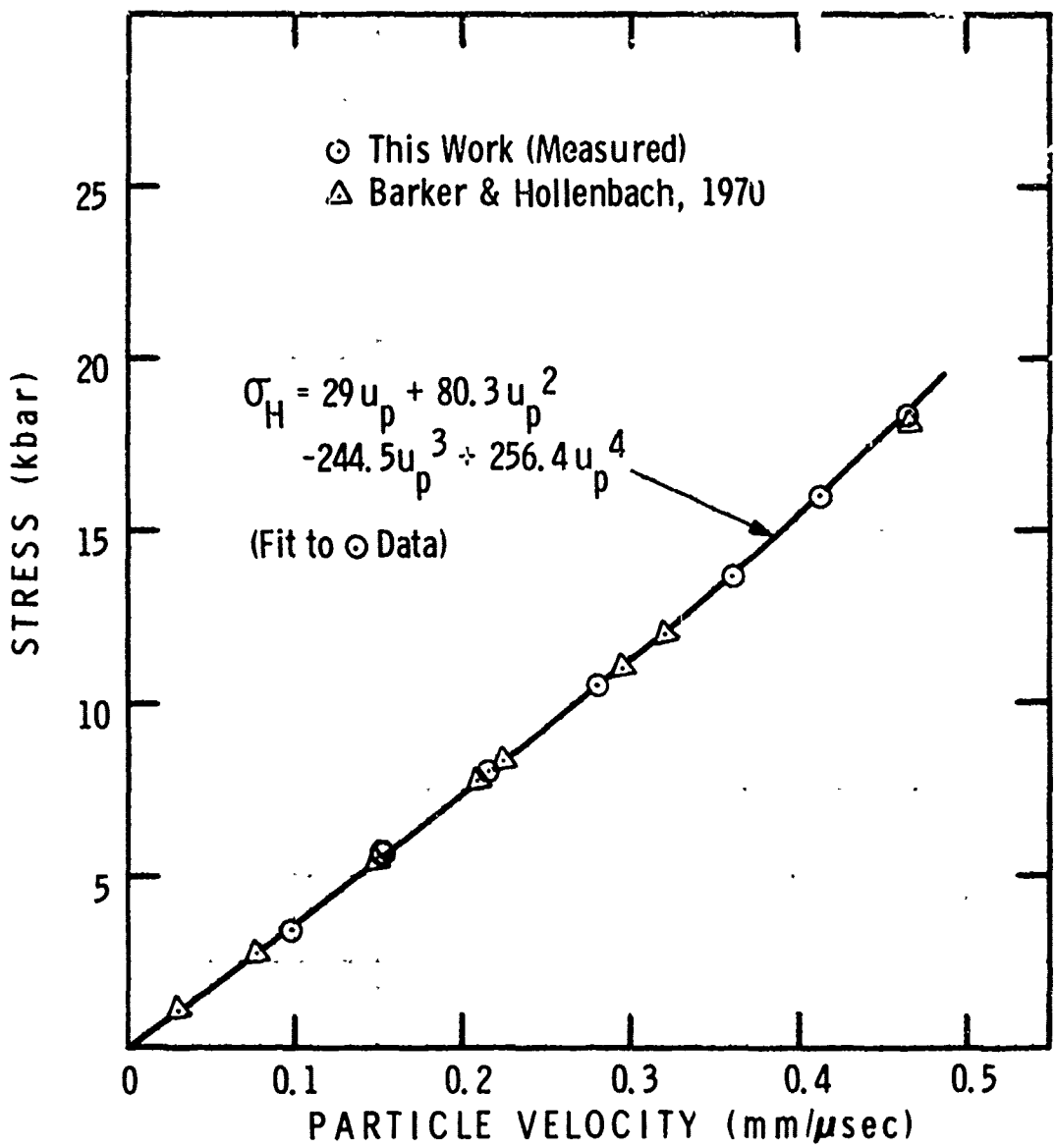

Figure 3 Stress-Particle Velocity Hugoniot, PMMA

TABLE II

HUGONIOT DATA, PMMA

Stress[1] (kbar)	Particle Velocity[1] (mm/μs)	Shock Velocity[2] (mm/μs)	Strain[2] $1-(v/v_o)$	Compression[2] $(v_o/v)-1$
3.40	0.099	2.90	0.0341	0.0353
5.55	0.151	3.11	0.0486	0.0511
8.04	0.214	3.18	0.0674	0.0723
10.6	0.280	3.20	0.0875	0.0959
13.7	0.359	3.23	0.111	0.125
16.0	0.414	3.27	0.127	0.145
18.4	0.468	3.32	0.141	0.164

1. Measured (quartz gages).
2. Calculated (ρ_o = 1.183 g/cc).

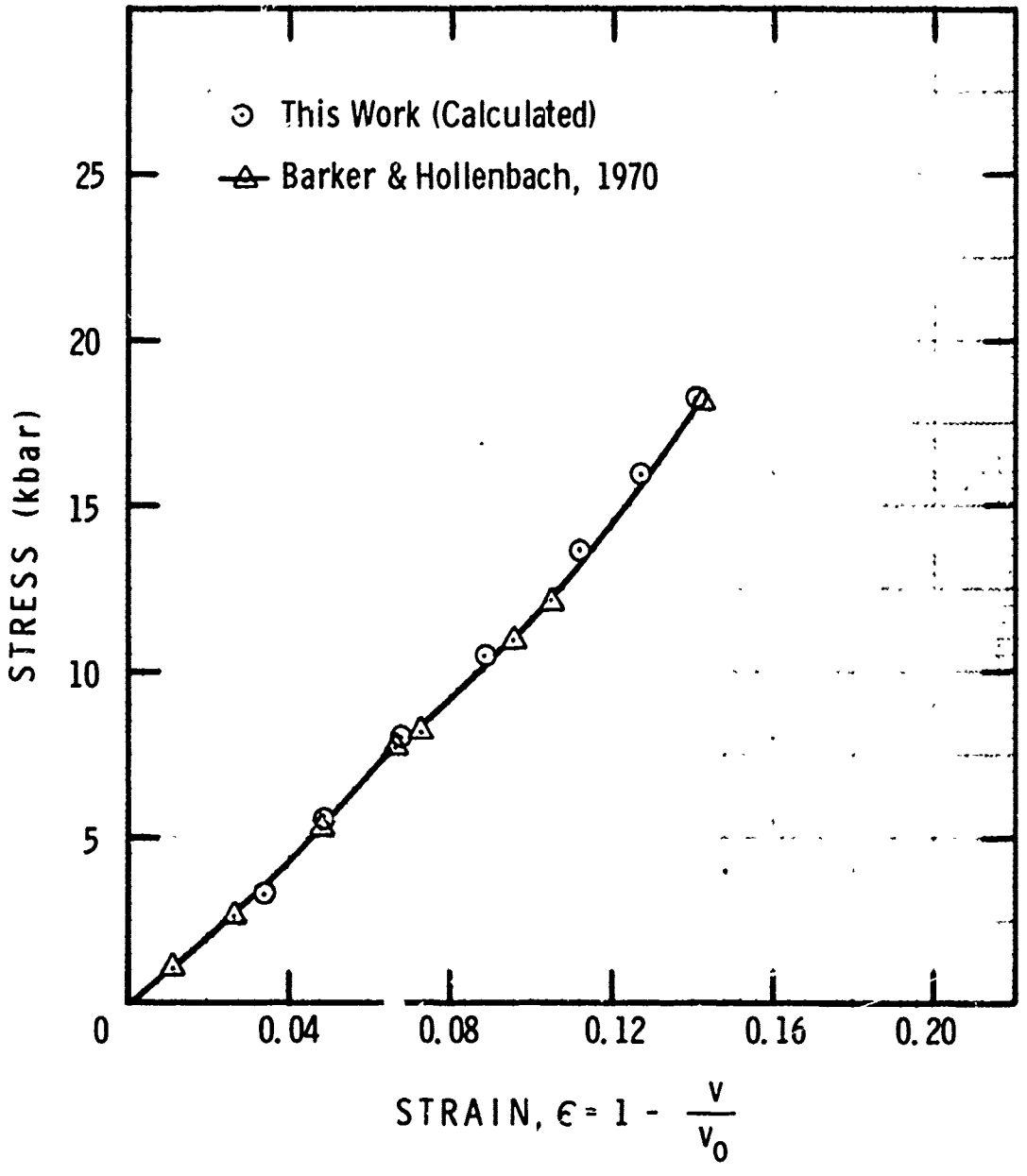

Figure 4 Stress-Strain Hugoniot, PMMA

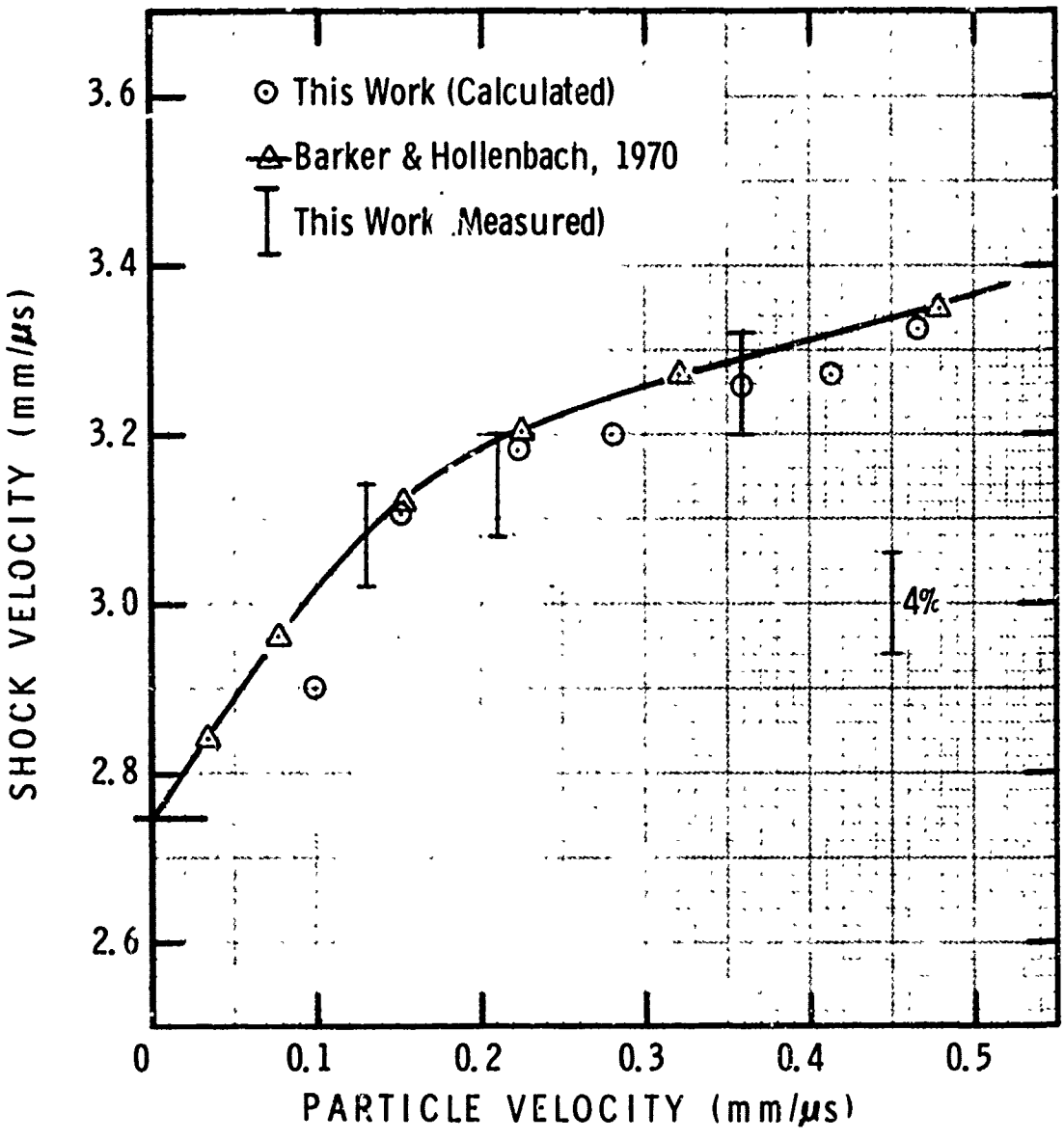

Figure 5 Shock Velocity-Particle Velocity Hugoniot, PMMA

The stress-compression hugoniot data are compared to ultrasonic hydrostats and hydrostatic compressibility in Figure 6. The ultrasonic hydrostats are based on Asay's pressure data and the equations of Birch,[24,25]

$$P_T = 84.6\ (1+\mu)^{7/3} - (1+\mu)^{5/3}\ 1+6.75\ (1+\mu)^{2/3} - 1 \qquad (5)$$

Murnaghan,[26]

$$P_S = 4.80\ (1+\mu)^{12.2} - 1 \qquad (6)$$

and Keane.[27,28]

$$P_S = 7.9\ \left[(1+\mu)^{9.5} - 1\right] - 16.7\ \ln\ (1+\mu) \qquad (7)$$

The hydrostatic compression curve is Bridgman's data[29] as reported by Halpin and Graham.[19] Corrections from isothermal (P_T) and adiabatic (P_S) conditions to the hydrostat are less than 1% at 20 kbar and have been neglected. Compared to metals,[2-5] the agreement between the shock wave data and the hydrostats is relatively poor in the low-pressure region. The ultrasonic and hydrostatic compression results, which are essentially "static" measurements, do not show the inflections in stress-compression behavior indicated by the dynamic shock wave measurements.

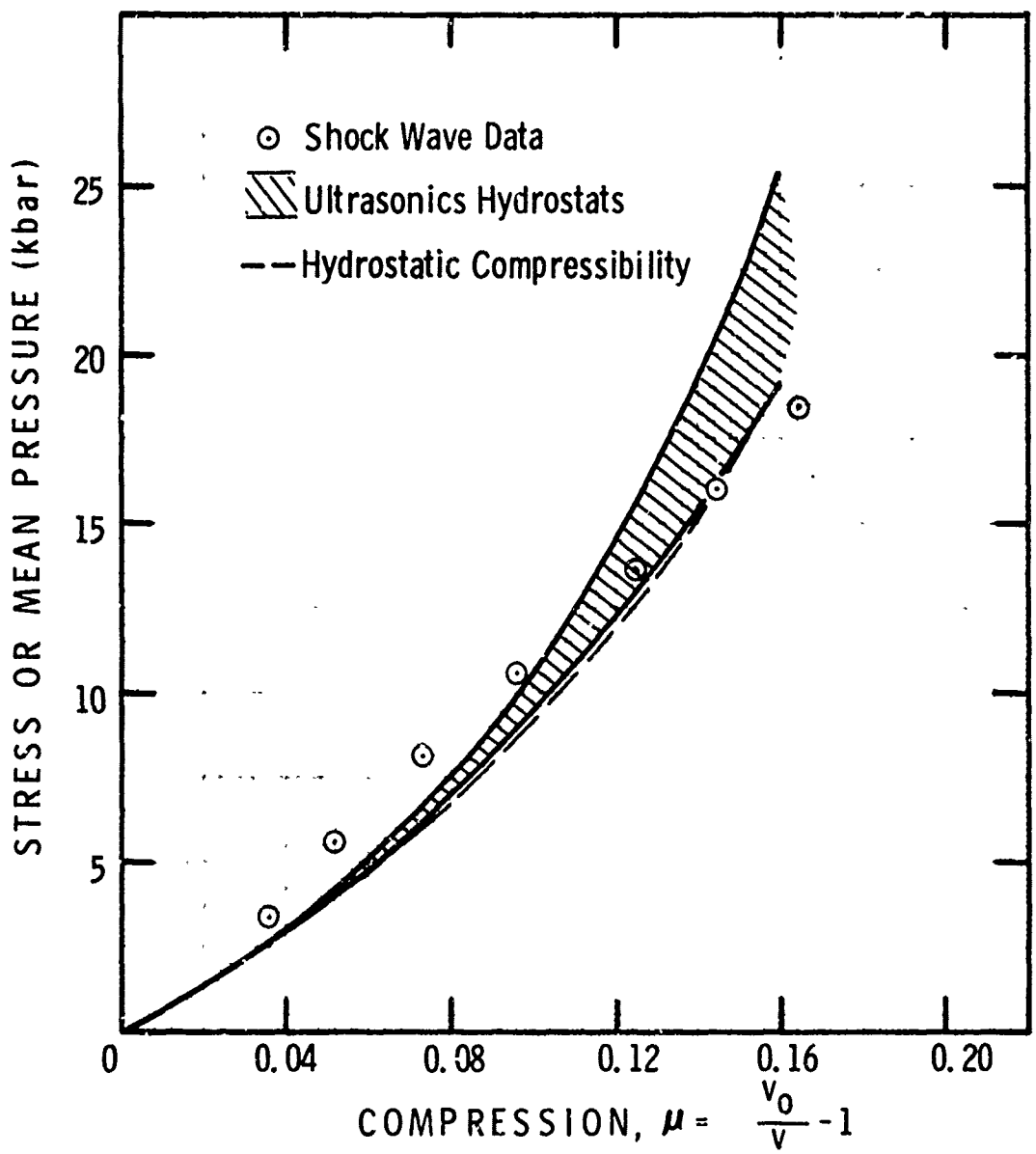

Figure 6 Stress-Compression Hugoniot, PMMA

SECTION IV

WAVE PROPAGATION

Shock wave characteristics were measured using quartz, a velocity interferometer and magnetic foil gages. The results presented here complement the more detailed work reported by Barker and Hollenbach[21] and Schuler[22] on the same grade of PMMA. They studied compressive and release wave characteristics at stresses up to 25 kbar and propagation distances out to 37 mm and also examined steady-state wave conditions.

Quartz gage records of compressive waves in PMMA at propagation distances of 3 and 6 mm are shown in Figure 7. The rise-time (after correcting for tilt effects) is only a few nanoseconds up to about two-thirds peak stress, after which there is a gradual rounding of the wave front for $\sim$ 0.5 μsec.

Representative records from the velocity interferometer and magnetic foil gage tests are given in Figure 8. Interferometer fringe patterns were generally clean and well-defined, giving good release wave arrival time and shape, although the compressive wave rise-time was too fast to permit fringe resolution. The magnetic foil gage test records were also noise-free but did show a slight "hump" at the first release level which has not been explained.

Velocity interferometer records are shown in Figure 9 with test conditions for each shot listed in Table III. The compressive behavior is essentially the same as described above although there is less rounding for the low velocity test (No. 95, $\sim$ 1.7 kbar). Spreading of the release wave with

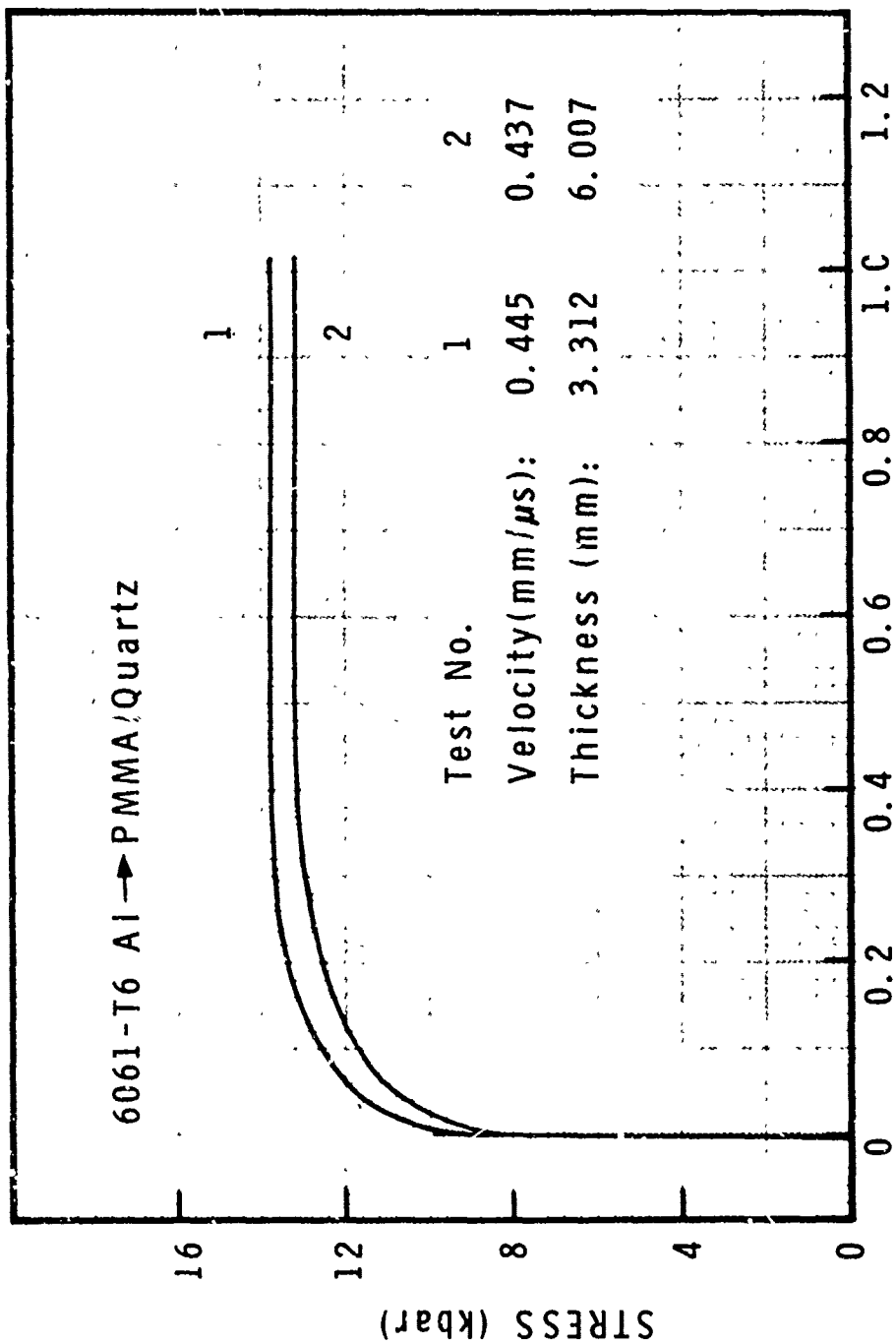

Figure 7 Compressive Waves in PMMA (X-Cut Quartz Gages)

VELOCITY INTERFEROMETER

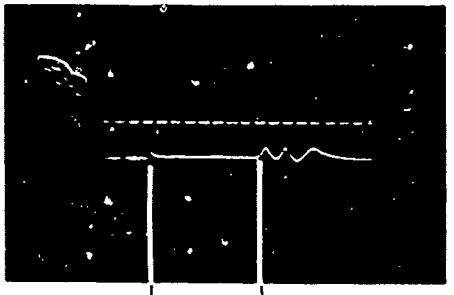

PMMA → PMMA/PMMA
V_I = 0.407 mm/μs
X = 3.414mm
σ_H = 7.5 kbar

MAGNETIC FOIL GAGE

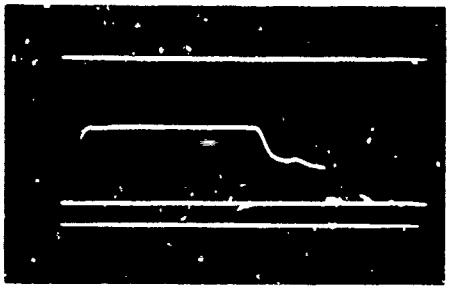

FQ → PMMA/M.F./PMMA
V_I = 0.163 mm/μs
X = 1.996mm
σ_H = 4.6 kbar

Figure 8 Wave Profile Test Records

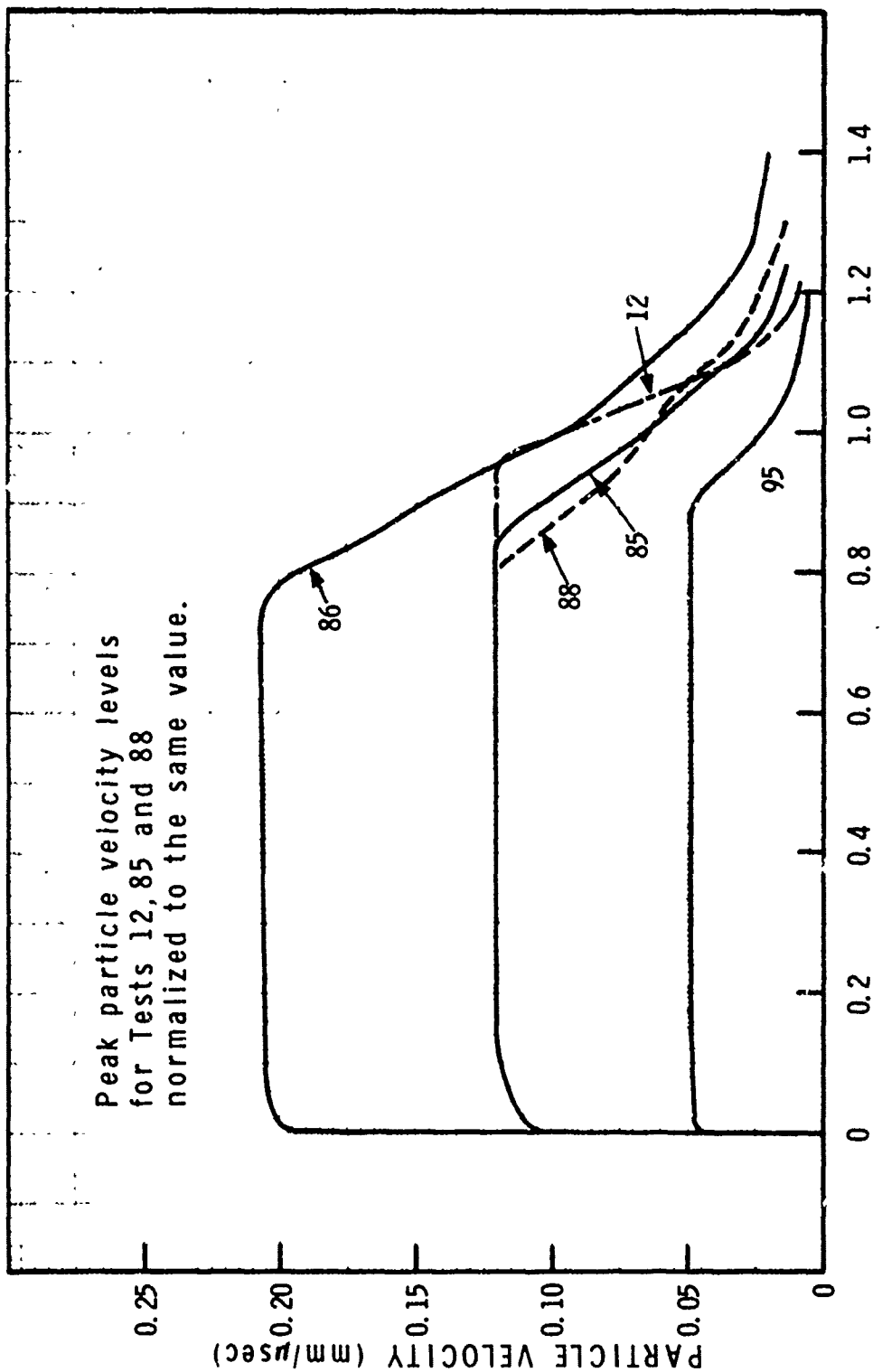

Figure 9 Wave Profiles in PMMA (Velocity Interferometer)

TABLE III

VELOCITY INTERFEROMETER TEST DATA

Test No.	V_I Impact Velocity (mm/μs)	Max. Stress (kbar)	X_o Impactor Thickness (mm)	X Target Thickness (mm)	X/X_o	Config.
12	0.277	5.0	1.651	1.473	0.89	PMMA→PMMA/PMMA
85	0.246	4.4	1.542	3.391	2.20	" "
86	0.407	7.5	1.527	3.414	2.24	" "
88	0.250	4.5	1.590	6.459	4.06	" "
89	0.256	4.6	1.463	3.269	2.23	PMMA→PMMA
95	0.097	1.7	1.433	3.332	2.33	PMMA→PMMA/PMMA

increasing propagation distance is evident and there is some indication of structure in the release wave, being more pronounced at the higher particle velocity (No. 86) and at the longer propagation distance (No. 88). Similar behavior was noted by Barker.[21]

The magnetic foil test consisted of a multi-layered target with foil gages at the impact surface (input) and at three propagation distances. Results are shown in Figure 10, with wave arrival times calculated on the basis of a constant shock velocity of 3.07 mm/μsec. The initial release wave does not reduce particle velocity to zero because the impedance of the fused quartz impactor is higher than that of PMMA. The input pulse is not perfectly square due to the effects of impact tilt and gage thickness effects. As noted for the interferometer tests, there is spreading of the release wave with propagation distance although peak particle velocity attenuation has not yet occurred at the maximum distance (12.63 mm) observed.

One wave profile test was conducted on a "designed-composite." This composite consisted of aluminum rods inserted and bonded into a PMMA matrix and the test configuration is shown schematically in Figure 11. The transmitted compressive wave was measured with a 12.7 mm thick quartz gage and the test result is given in Figure 12 in terms of quartz stress. The initial portion of the wave is due to propagation down the aluminum rods and the slight structure evident in the first 0.8 μsec is probably due to elastic-plastic effects in aluminum. Arrival of the wave propagating in the matrix gives a final stress jump to ∿ 11 kbar. Wave transit times in the rods and the matrix corresponded to the elastic wave velocity in aluminum and shock wave velocity in PMMA, respectively.

MSL-71-24

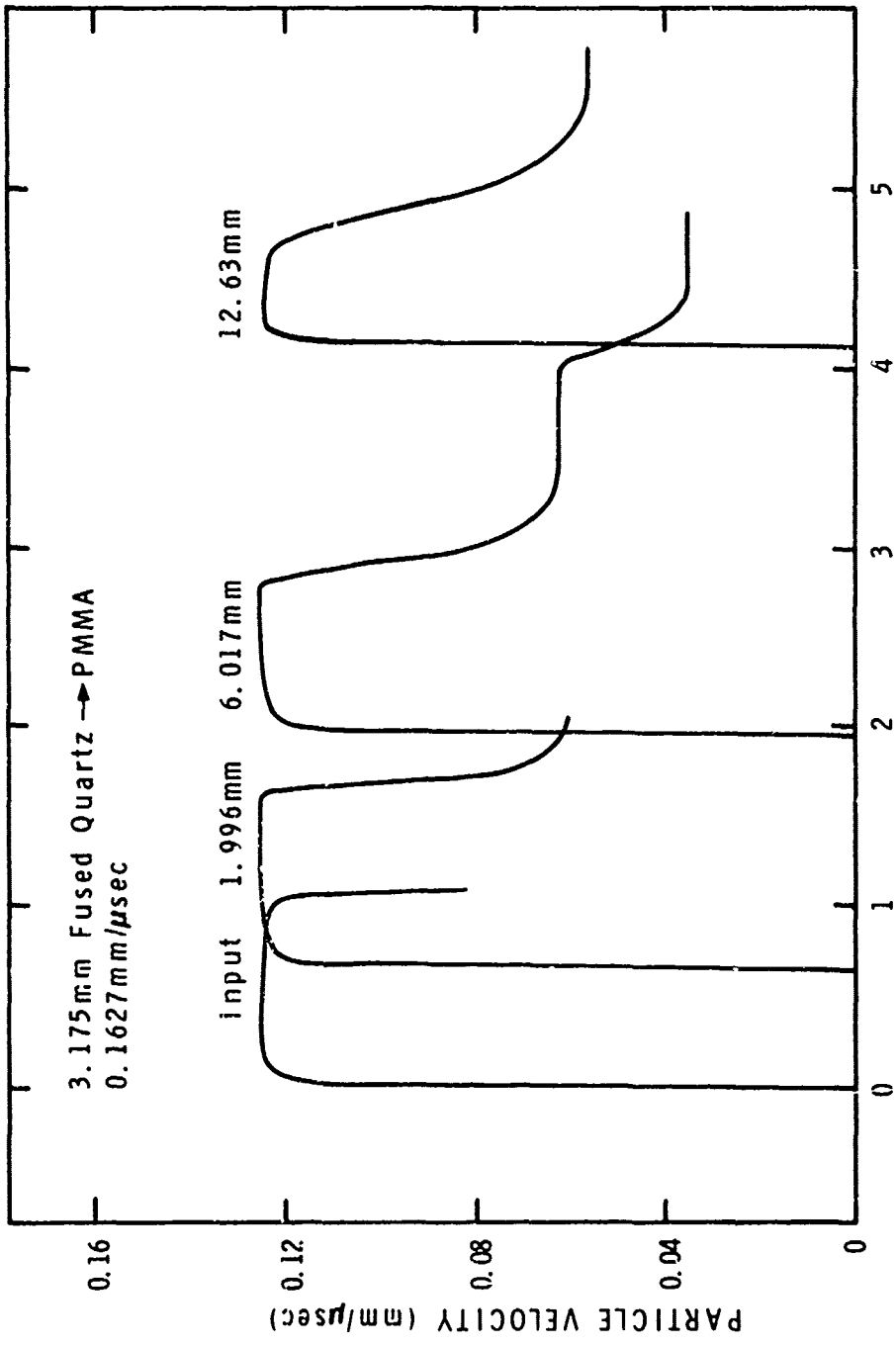

Figure 10 Wave Profiles in PMMA (Magnetic Foil Gages)

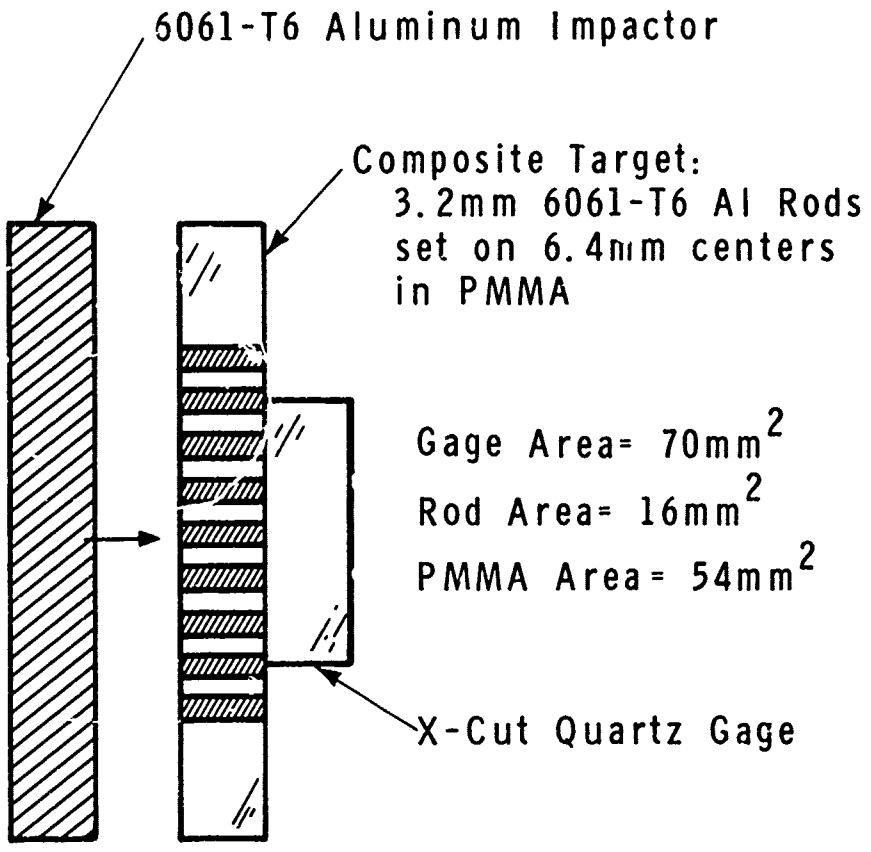

Figure 11 Designed Composite, Test Configuration

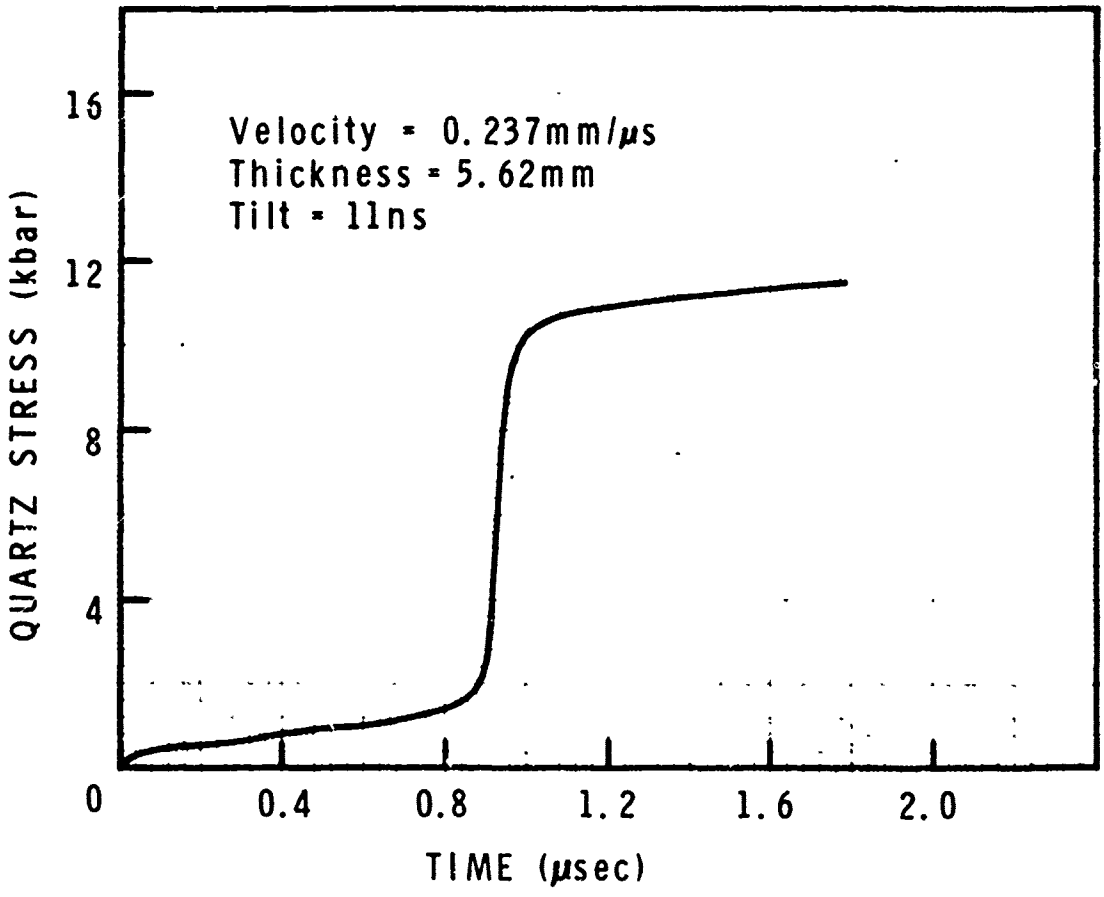

Figure 12 Compressive Wave in Designed Composite

SECTION V

SPALL FRACTURE

RECOVERY TESTS

Spall behavior of PMMA was studied by carrying out a series of impact and recovery tests.* Unlike metals, the recovered specimens did not require sectioning and metallographic preparation to determine the presence of fractures. Spall damage could be observed simply by viewing the specimen in transmitted light parallel to the shock wave propagation direction. However, the onset of spall in PMMA was evidenced by the appearance of one or a few "penny-like" cracks several millimeters in diameter, rather than numerous small voids or cracks. This, together with poor reproducibility apparently due to material effects, made determination of an incipient spall level even more difficult than with metals.

Incipient spall results for three times of loading (i.e., three impactor thicknesses), are given in Figure 13, along with earlier spall data of Charest[32] and Keller[33]. The present data show a dependence of incipient spall velocity on time of loading. This is in agreement with the results of Charest who also used a gun-launched flat-plate technique. Keller showed a time-independent behavior, however, his data are for an exploding-foil technique. All three sets of data show different incipient spall levels, which is probably due to a number of factors, the most important of which are material variability, influence of differences in the X/X_o ratio, and different incipient spall criteria.

* The fracture of PMMA under uniaxial stress conditions has been studied in detail by Beardmore and Johnstone.[30,31]

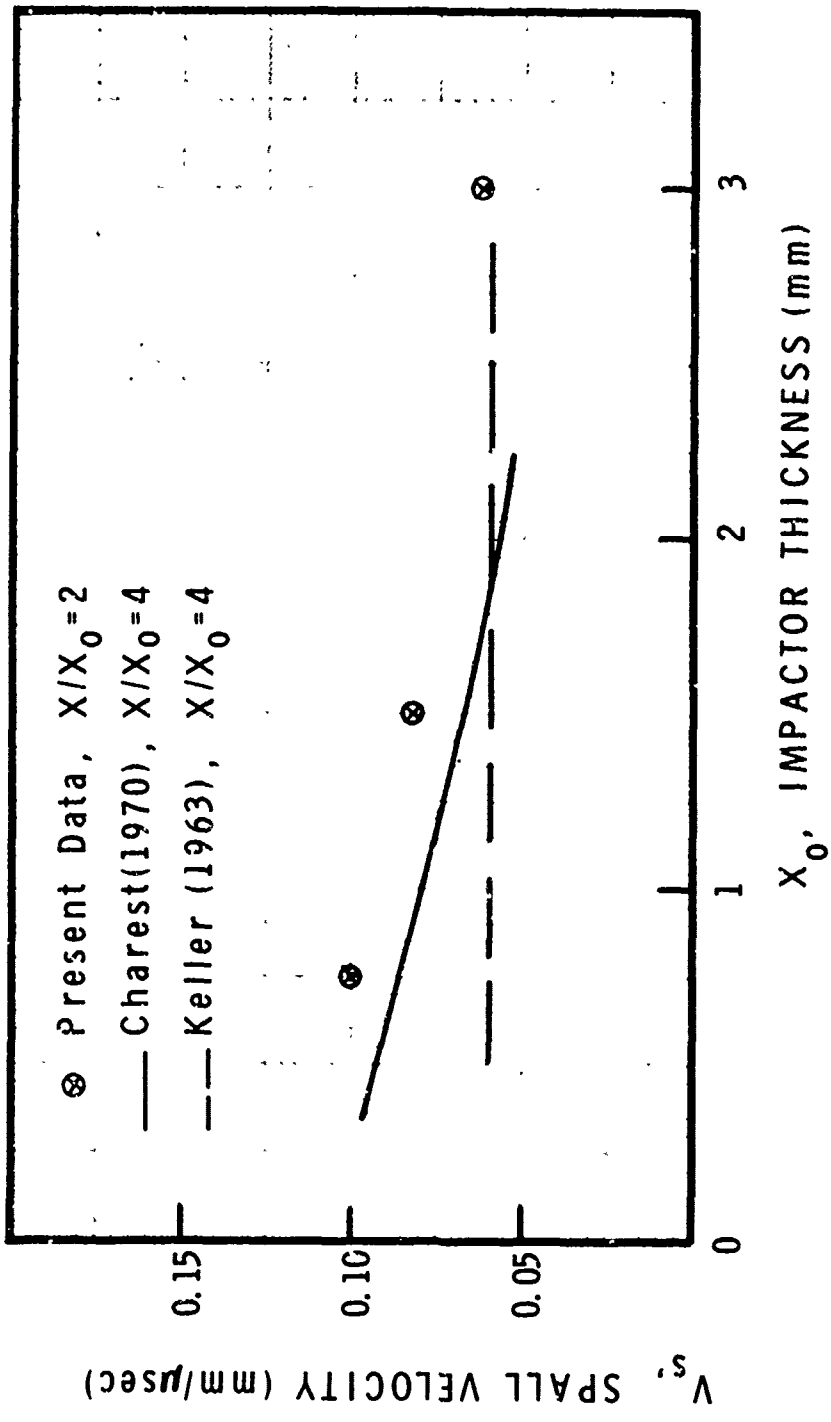

Figure 13 Spall Data for PMMA

Fractures appearing at the incipient spall level are difficult to photograph optically because of depth of field problems and the relatively small difference in light transmission characteristics between incipient fractures and unfractured material. Optical photographs of specimens from tests ∿ 10% above the incipient spall level are shown in Figure 14. (The dark "shadow" in the center of the righthand picture is a crack extending from the specimen surface to the spall plane). Although, of approximately the same total area, the fracture region has a considerably different appearance for the two specimens, the reason for which is not understood.

An optical photomicrograph of a completely spalled specimen is shown in Figure 15. The fracture surface has the appearance of a "polycrystalline" structure with extensive cracking or crazing within the "grains". The fracture subsurfaces were generally flat and normal to the shock propagation direction, although they were not all in the same plane (dispersion of ∿ 0.2 mm). A scanning electron micrograph of the same specimen is shown in Figure 16.

A spall test was performed on a sample of FF-17 phenolic being studied under a related program.[34] This material is a cured phenolic resin with a density of 1.29 g/cc. The specimen was completely spalled and the resulting fracture surface is shown in Figures 17 and 18. The optical photomicrographs (Figure 17) indicate that fracture initiated at a large number of points or defects and then propagated radially from these points, giving a "sunburst" pattern. These fracture zones were typically 0.1 to 0.4 mm diameter and, like PMMA, were generally flat and normal to the shock propagation direction. The scanning microfractographs show in more detail the development of this pattern around the central initiation point.

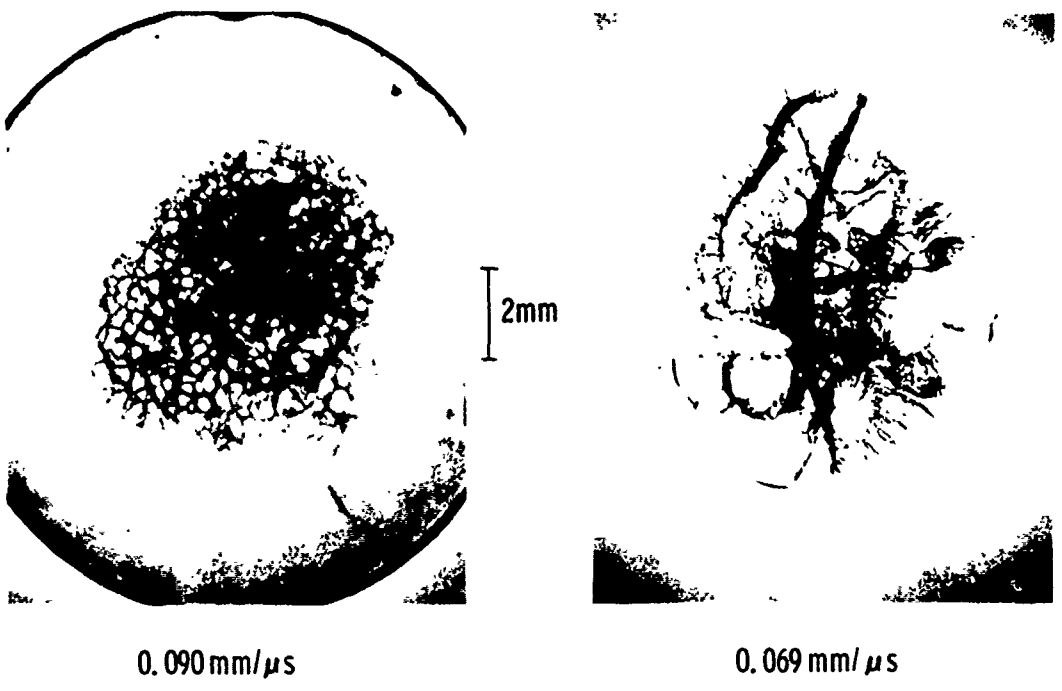

Figure 14 Spall Fractures in PMMA

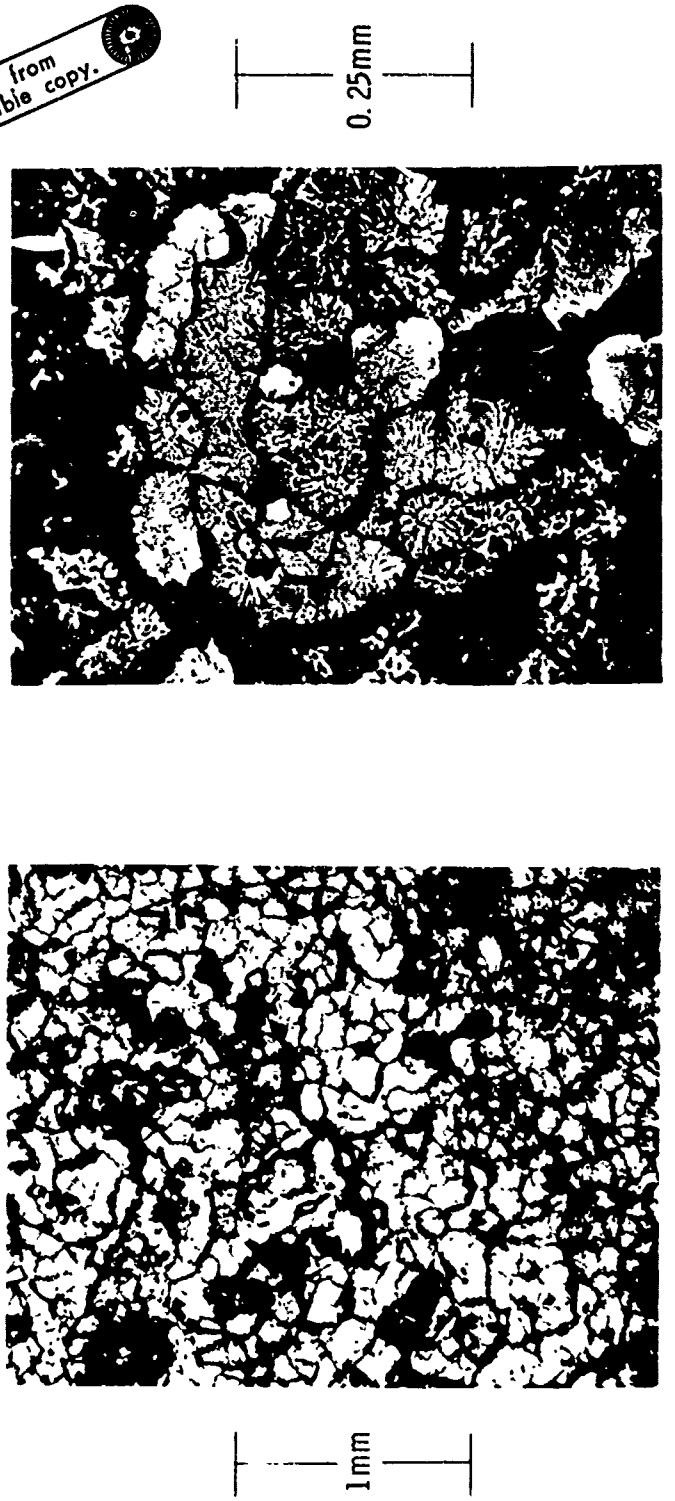

Figure 15 Spall Fracture Surface in PMMA (1.5 mm + 3.00 mm, 0.157 mm/μsec)

SPUTTERED 0.4μm GOLD SURFACE

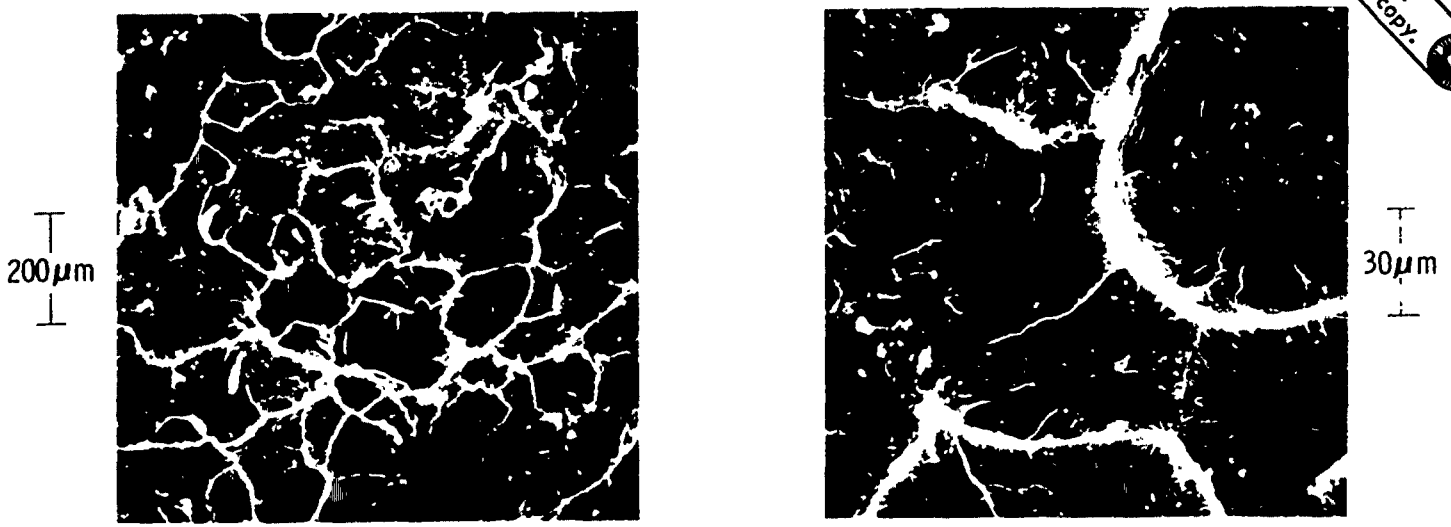

Figure 16 Spall Fracture Surface in PMMA, Scanning Microfractograph, 0° (1.5 mm → 3.0 mm, 0.157 mm/μsec)

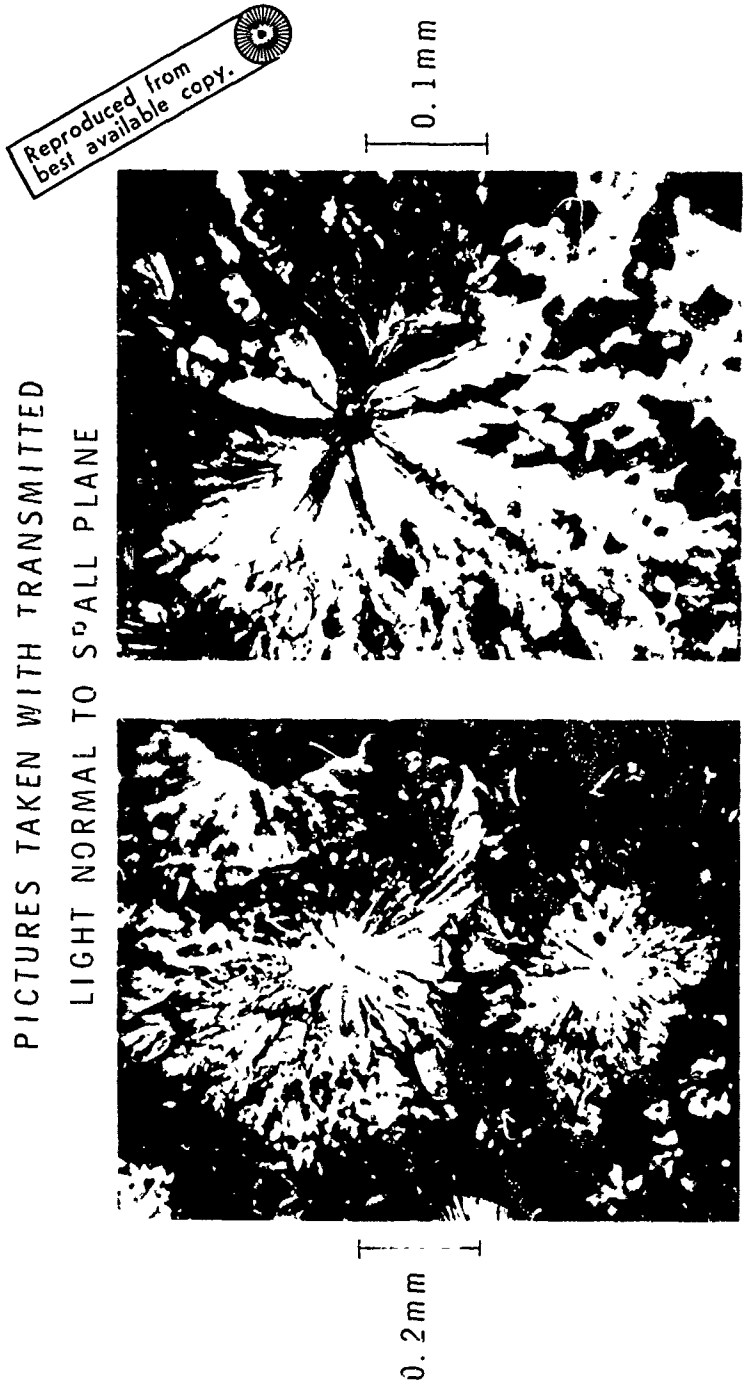

Figure 17 Spall Fracture Surfaces in FF-17 Phenolic

MSL-71-24

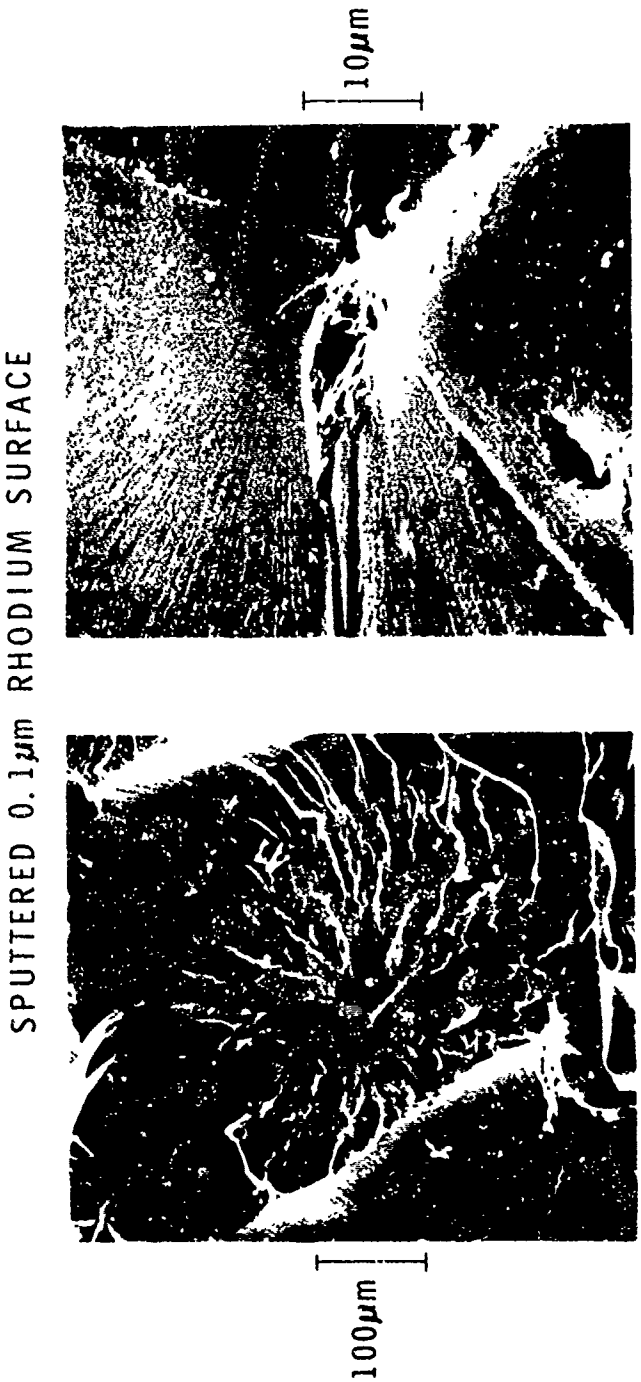

Figure 18 Spall Fracture Surface in FF-17 Phenolic, Scanning Microfractograph, 45°

SPALL WAVE PROFILE

One test was conducted to obtain a complete wave profile under spall-producing conditions and the result is shown in Figure 19 (see Table III for test conditions). A good, noise-free velocity interferometer record was obtained, however, analysis of this record was difficult in that the expected wave profile is not entirely consistent with the apparent fringe pattern.* The compressive wave and release wave arrival are clear and agree with the wave profiles discussed earlier. The fringe pattern does not give an obvious fringe reversal after release wave arrival and therefore several interpretations of the release path are possible. The solid line shown implies a reversal at point A, which gives a pullback or release wave reversal[36] of ∿ 0.07 mm/μsec. This pullback is related to the spall strength of the material, and for metals[2-5] it is always less than the incipient spall velocity for a given set of impact conditions. For the conditions shown, the incipient spall velocity in PMMA is ∿ 0.08 mm/μsec, which supports assumption of a reversal point at A. The dashed line is for no reversal at A Although there is a fringe beginning at point B, the absence of a reversal between A and B would give a wave profile beyond B that is not reasonable. The solid wave would continue up above the initial peak velocity level while the dashed curve would continue down towards zero velocity, neither of which is consistent with observed spall profile behavior for other materials.

* Barker gives a detailed discussion of fringe analysis in Referencer 20 and 35.

MSL-71-24

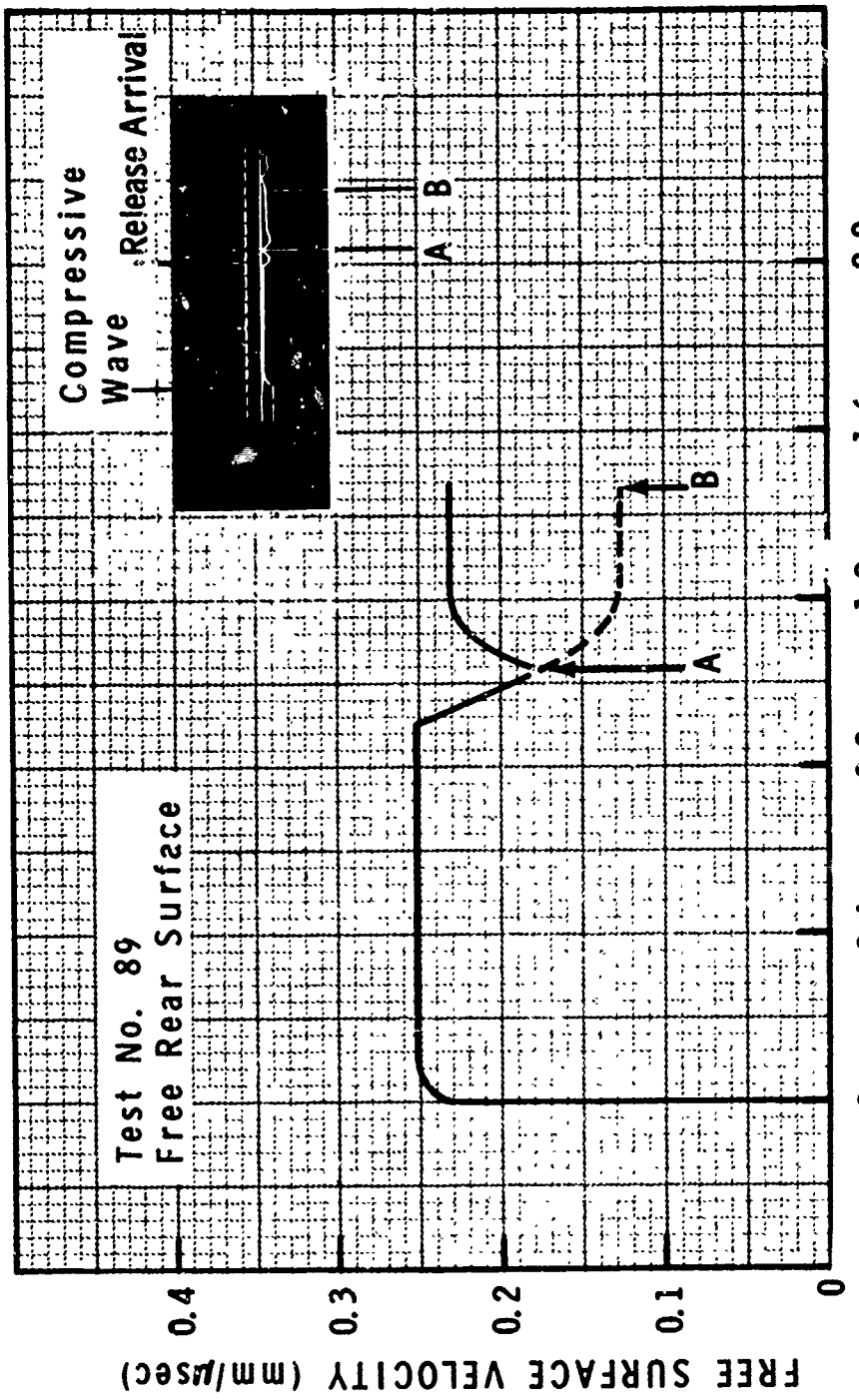

Figure 19 Spall Wave Profile in PMMA

REFERENCES

1. Isbell, W. M., Christman, D. R., Babcock, S. G., Michaels, T. E. and Green, S. J., "Measurements of Dynamic Properties of Materials, Vol. I: Summary of Results," General Motors Corporation, Manufacturing Development, DASA 2501-1, 1970 (AD712847).

2. Christman, D. R., Isbell, W. M., Babcock, S. G., McMillan, A. R. and Green, S. J., "Measurements of Dynamic Properties of Materials, Vol. III: 6061-T6 Aluminum," General Motors Corporation, Manufacturing Development, DASA 2501-3, 1971.

3. Christman, D. R., Michaels, T. E., Isbell, W. M. and Babcock, S. G., "Measurements of Dynamic Properties of Materials, Vol. IV: Alpha Titanium," General Motors Corporation, Manufacturing Development, DASA 2501-4, 1971.

4. Christman, D. R., Isbell, W. M. and Babcock, S. G., "Measurements of Dynamic Properties of Materials, Vol. V: OFHC Copper," General Motors Corporation, Manufacturing Development, DASA 2501-5, 1971 (AD728846).

5. Isbell, W. M., Christman, D. R. and Babcock, S. G., "Measurements of Dynamic Properties of Materials, Vol. VI: Tantalum," General Motors Corporation, Manufacturing Development, DASA 2501-6, 1971.

6. Christman, D. R., Isbell, W. M., Babcock, S. G., McMillan, A. R. and Green, S. J., "Measurements of Dynamic Properties of Materials, Vol. II: Experimental Methods and Techniques," General Motors Corporation, Manufacturing Development, DASA 2501-2, 1971 (AD730750).

7. Data Sheet PL-229k, Rohm and Haas, Philadelphia, Pa., 1967.

8. Asay, J. R., Urzendowski, S. R. and Guenther, A. H., "Ultrasonic and Thermal Studies of Selected Plastics, Laminated Materials, and Metals," Air Force Weapons Laboratory, AFWL-TR-67-91, January, 1968 (AD 827596).

9. Thermophysical Properties of High Temperature Solid Materials, Volume 6: Intermetallics, Cermets, Polymers, and Composite Systems, Part II (Plexiglas, p. 1020-1029), The McMillan Co., New York, 1967.

10. Maiden, C. J. and Green, S. J., "Response of Materials and Structures to Suddenly Applied Stress Loads (Phase I)," General Motors Corporation, GM Defense Research Laboratories, DASA 1716, October, 1965 (AD 476613).

11. Green, S. J., et al, "Fundamental Material Behavior Study," General Motors Corporation, GM Defense Research Laboratories, BSD TR 66-398, October, 1966 (AD 804889L).

12. Green, S. J., Babcock, S. G. and Perkins, R. D., "Response of Several Reentry Vehicle Materials to Impulsive Loads," General Motors Corporation, AC Electronics-Defense Research Laboratories, BSD-TR-67-23, February, 1967 (AD 822803L).

13. Babcock, S. G., Kumar, A. and Green, S. J., "Response of Materials to Suddenly Applied Stress Loads, Part I: High Strain-Rate Properties of Eleven Reentry-Vehicle Materials at Elevated Temperatures," General Motors Corporation, Manufacturing Development, AFFDL-TR-67-35, Part I, April, 1967 (AD 813880).

14. Holt, D. L., "The Modulus and Yield Stress of Glassy Poly(methylmethacrylate) at Strain Rates up to 10^3 Inch/Inch/Second," J. Appl. Polymer Sci., Vol. 12, 1968, p. 1653-1659.

15. Ender, D. H., "Stress Softening and Strain Softening of Poly(methylmethacrylate) in Yielding under Constant Load," J. Appl. Phys., Vol. 39, 1968, p. 4877-4882.

16. Duckett, R. A., Rabinowitz, S. and Ward, I. M., "The Strain-rate, Temperature and Pressure Dependence of Yield of Isotropic Poly(methymethacrylate) and Poly(ethylene terephthalate)," J. Mat. Sci., Vol. 5, 1970, p. 909-915.

17. Asay, J. R., Lamberson, D. L. and Guenther, A. H., "Pressure and Temperature Dependence of the Acoustic Velocities in Poly(methylmethacrylate)," J. Appl. Phys., Vol. 40, 1969, p. 1768-1783.

18. Liddiard, T. P., "The Compression of Poly(methylmethacrylate) by Low Amplitude Shock Waves," Proc. Fourth Symp. on Detonation, ACR-126, U.S. Government Printing Office, October, 1965, p. 214-221.

19. Halpin, W. J. and Graham, R. A., "Shock Wave Compression of Plexiglas from 3 to 20 kilobars," Proc. Fourth Symp. on Detonation, ACR-126, U.S. Government Printing Office, October, 1965, p. 222-232.

20. Schmidt, D. N. and Evans, M. W., "Shock Wave Compression of Plexiglas in the 2.5 to 20 Kilobar Region," Nature, Vol. 206, 1965, p. 1348-1349.

21. Barker, L. M. and Hollenbach, R. E., "Shock-Wave Studies of PMMA, Fused Silica, and Sapphire," J. Appl. Phys., Vol. 41, 1970, p. 4208-4226.

22. Schuler, K., "Propagation of Steady Shock Waves in Poly(methylmethacrylate)," J. Mech. Phys. Solids, Vol. 18, 1970, p. 277-293.

23. Deal, W. E., "Shock Wave Research on Inert Solids," Proc. Fourth Symp. on Detonation, ACR-126, U.S. Government Printing Office, October, 1965, p. 321-345.

24. Birch, F., "The Effect of Pressure Upon the Elastic Parameters of Isotropic Solids, According to Murnaghan's Theory of Finite Strain," J. Appl. Phys. Vol. 9, p. 279-288, 1938.

25. Birch, F., "Elasticity and Constitution of the Earth's Interior," J. Geophys. Res., Vol. 57, p. 227-286, 1952.

26. Murnaghan, F. D., "The Compressibility of Media Under Extreme Pressures," Proc. Nat. Ac. Sci., Vol. 30, p. 244-247, 1944.

27. Keane, A., "An Investigation of Finite Strain in an Isotropic Material Subjected to Hydrostatic Pressure and its Seismological Applications," Australian J. Phys., Vol. 7, p. 323-333, 1954.

28. Anderson, O. L., "On the Use of Ultrasonic and Shock-Wave Data to Estimate Compressions at Extremely High Pressures," Phys. Earth Planet. Interiors, Vol. 1, p. 169-176, 1968.

29. Bridgman, P. W., "Pough Compression of 177 Substances to 40,000 kg/cm^2," Paper No. 161, Collected Experimental Papers, Vol. VI, p. 3835-3851, Harvard University Press, Cambridge, Mass., 1964.

30. Beardmore, P. and Johnstone, T. L., "Fracture of Poly(methylmethacrylate) at Low Temperatures," Phil. Mag., Vol. 23, p. 1119-1131, 1971.

31. Beardmore, P., "Temperature Dependence of Yield and Fracture in Poly(methylmethacrylate)," Phil. Mag., Vol. 19, p. 389-401, 1967.

32. Charest, J. A., Horne, D. E. and Jenrette, B. D., "Phenomenological Considerations for Spall Measurements," EG&G, Santa Barbara Division, S-56-TP, January, 1970.

33. Keller, D. V. and Trulio, J. G., "Mechanism of Spall in Lucite," J. Appl. Phys., Vol. 34, 1963, p. 172-175.

34. Michaels, T. E., Christman, D. R. and Isbell, W. M., "Experimental Wave Propagation Studies in Composite Materials," General Motors Corporation, Manufacturing Development, AFWL-TR-71-153, December, 1971.

35. Barker, L. M., "Fine Structure of Compressive and Release Wave Shapes in Aluminum Measured by the Velocity Interferometer Technique," Behavior of Dense Media under High Dynamic Pressures, p. 483-505, Gordon and Breach, New York, New York, 1968.

36. Isbell, W. M. and Christman, D. R., "Shock Propagation and Fracture in 6061-T6 Aluminum from Wave Profile Measurements," General Motors Corporation, Manufacturing Development, DASA 2419, April, 1970 (AD 705536).